AIAA JOURNAL
Vol. 34, No. 8, August 1996

Heuristic Method for Evaluating Coil Performance

John Hon*
Rockwell International/Rocketdyne, Canoga Park, California 91304
D. N. Plummer,† P. G. Crowell,† and J. Erkkila†
Logicon RDA, Albuquerque, New Mexico 87119
and
G. D. Hager,‡ C. Helms,§ and K. Truesdell¶
U.S. Air Force Phillips Laboratory, Kirtland Air Force Base, New Mexico 87117-5776

A heuristic methodology is described that was developed to evaluate the chemical efficiency of high-power chemical oxygen iodine laser (COIL) devices and its application to the specific evaluation of the U.S. Air Force Phillips Laboratory's RotoCOIL laser. A heuristic equation that forms the basis of this methodology and describes the COIL energy flow, energy losses, and power extraction using measured data, code results, and empirical relations is presented. Using this equation and bounding values for some of its terms, it is shown that for the RotoCOIL performance data the experimentally measured average $O_2(^1\Delta)$ yield of 0.40 is nearly 38% below that which would be consistent with the measured extraction power. By relating terms of the heuristic equation to performance of individual components of the COIL system, it is concluded that nearly 50% of the efficiency loss for the RotoCOIL laser derives from oxygen generator and delivery losses, whereas 15% is from nozzle inefficiencies and 11% from resonator losses.

Nomenclature

A = cross-sectional flow area in the optical cavity
A_{out}, A_{max} = mode footprint area at outcoupler and maximum reflectivity mirrors
$\dot{Cl}_2$ = chlorine flow rate into generator, mole/s
F = iodine dissociation fraction
G_o = average small signal gain in direction of optical axis
G_{th} = threshold gain
$\dot{I}_2$ = iodine flow rate
K_{deact} = rate coefficient for quenching of I* by H_2O
K_g = defined by Eq. (15)
k_{eq} = equilibrium constant for I atom pumping reaction, Eq. (5)
k_F, k_R = rate coefficients for I atom pumping reaction, Eq. (5), and reverse reaction, Eq. (6)
k_1 = chlorine utilization rate parameter, defined in Ref. 14
k_3 = $O_2(^1\Delta)$ production rate parameter, defined in Ref. 14
L_g = gain length
L_m = length of the optical extraction mode in the flow direction, cm
N = number of singlet delta oxygen molecules to dissociate an iodine molecule
N_A = Avogadro's number
P_{av} = power available in cavity
P_{out} = power extracted from resonator
$\mathcal{P}$ = fraction of the outcoupled power lost as a result of diffraction effects
R_{out}, R_{max} = mirror reflectivities for resonator output and maximum reflectivity mirrors
S_{out}, S_{max} = mirror scattering losses for resonator output and maximum reflectivity mirrors
T_{cav} = static cavity gas temperature
T_{cavo} = static cavity gas temperature with no dissociation
U_{Cl_2} = chlorine utilization defined by Eq. (3)
v = average flow velocity
x_{ef} = e-folding length for the reduction of $O_2(^1\Delta)$ during power extraction
Y = singlet delta oxygen yield defined by Eq. (4)
Y_{cav} = singlet delta yield in cavity
Y_{deact} = singlet delta yield loss as a result of water deactivation of I* in laser cavity
Y_{diss} = singlet delta yield loss during dissociation
Y_{plen} = singlet delta yield just upstream of the I_2 injection
Y_{th} = minimum singlet delta yield for positive gain
γ_w = heterogeneous quenching probability of $O_2(^1\Delta)$ on basic hydrogen peroxide
η_{chem} = overall chemical efficiency of laser defined by Eq. (1)
η_{ext} = optical extraction efficiency
η_{extm} = medium extraction efficiency
η_{extr} = resonator extraction efficiency
η_{geo} = fraction of flow interrogated by resonator normal to the flow and optic axis
η_{mix} = accessed $O_2(^1\Delta)$/total $O_2(^1\Delta)$
η_{res} = flow residence time efficiency
σ = gain cross section
ϕ = COIL chemistry parameter defined by Eq. (28)
91 = lasing energy of 1 mole of I*, kJ
[ ] = species concentration in number per cubic centimeter

Presented as Paper 94-2422 at the AIAA 25th Fluid Dynamics, Plasmadynamics, and Lasers Conference, Colorado Springs, CO, June 20–23, 1994; received Oct. 17, 1995; revision received April 6, 1996; accepted for publication April 14, 1996.

*Consultant, Advanced Programs, Rocketdyne Division.
†Member, Technical Staff, Systems Technology Operation.
‡Technical Advisor, Applied Laser Technology Branch, Lasers and Imaging Directorate.
§Research Chemist, Applied Laser Technology Branch, Lasers and Imaging Directorate.
¶Branch Chief, Applied Laser Technology Branch, Lasers and Imaging Directorate.

I. Introduction

CHEMICAL oxygen–iodine laser (COIL) device technology has advanced steadily over the last 10 years. Table 1 shows a partial, chronological listing of reported performance for a number of devices. It is mostly restricted to larger, supersonic devices generating power in the range of kilowatts to tens of kilowatts. It shows a simple overall chemical efficiency η_{chem} defined as

$$\eta_{chem} = \frac{P_{out}}{91\dot{Cl}_2} \tag{1}$$

Table 1 **COIL chemical efficiency performance history**

Year	Ref.	Location[a]	Efficiency
1984	1	USA (AFWL)	0.116
1984	2	USA (AFWL)	0.147
1985	3	USA (RD)	0.138
1987	4	USA (AFWL)	0.175
1988	5	USA (AFWL)	0.231
1989	6	USA (AFWL)	0.236
1989	7	USA (RD)	0.209
1995	8	Russia	0.1
1991	9	USA (PL)	0.181
1995	10	Israel	0.05
1993	11	USA (PL)	0.134

[a]AFWL = Air Force Weapons Laboratory, RD = Rockwell International/Rocketdyne, and PL = Phillips Laboratory.

where the outcoupled power P_{out} is compared with the total device chlorine flow $\dot{C}l_2$ in mole/second. The factor 91 is the energy, in kilojoules, for one mole of iodine atoms, the lasing species, in the upper level of the lasing transition. This is an overall, end to end, all inclusive assessment parameter, the elements of which will be discussed later. The energy of singlet delta oxygen, 94.4 kJ/mole, is not utilized in this efficiency factor. This 4% loss is inherent in transferring this energy to atomic iodine in the COIL concept (i.e., the pumping reaction is slightly exothermic).

Table 1 shows that the best efficiency for any device of size is 0.24 for RotoCOIL. The obvious question is: where has the energy gone? What happened to 75% of the chemical energy? It is the purpose of this paper to answer this question as well as possible in view of incomplete and sometimes suspect data.

II. Heuristic Equation

The heuristic equation to be developed is based upon tracking the energy in a COIL device, starting with the incoming Cl_2 flow and ending with the outcoupled optical power, accounting for the losses along the way.

Heuristic Equation Development

Figure 1 shows a schematic of a generalized COIL device. The flow is from left to right. A mixture of chlorine and helium is introduced into an oxygen generator, where it contacts basic hydrogen peroxide (BHP). In the case of the RotoCOIL device, the generator is an assembly of thin disks that rotates into a bath of BHP and then picks up a thin film of liquid as it is rotated out of the BHP into the chlorine/helium flow. The overall reaction that takes place on the film is

$$Cl_2 + 2KO_2H \rightarrow O_2(^1\Delta) + H_2O_2 + 2KCl \tag{2}$$

This reaction produces excited oxygen, ground state oxygen, and, because the reaction is not complete, some residual chlorine. Also, because the film surface heats up because of the reaction, some water vapor is produced.

The efficiency of using chlorine is called the utilization U_{Cl_2}:

$$U_{Cl_2} = 1 - \frac{\text{residual chlorine}}{\text{total chlorine}} \tag{3}$$

The efficiency in generating excited oxygen is called yield Y:

$$Y = \frac{\text{excited oxygen}}{\text{total oxygen}} = \frac{O_2(^1\Delta)}{O_{2\,\text{total}}} \tag{4}$$

Usually the flow then passes through a cold trap, as shown, to reduce the water content. From the cold trap the flow is ducted to the subsonic entrance channel of the nozzle. In RotoCOIL, I_2 is injected as shown in Fig. 2. In subsequent processes the I_2 is dissociated. This uses some of the excited oxygen. From a macroscopic point of view, during dissociation N molecules of excited oxygen have been expended to dissociate one molecule of I_2. From energy considerations, N must be at least 2. Because some of the excited species participating in the dissociation process are deactivated during the process, N becomes larger than 2. The excited oxygen lost during dissociation is accounted for by Y_{diss}.

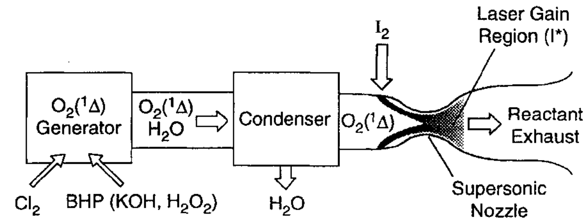

Fig. 1 Supersonic oxygen–iodine chemical laser concept.

The flow is then expanded supersonically into the optical cavity. During the supersonic expansion, energy is transferred to iodine atoms from excited oxygen to provide gain and power. As optical power is coupled out, repumping of the I atoms occurs. This process continues as long as there is gain and as long as the flow is in the optical mode.

Maintenance of positive gain is dependent upon maintaining sufficient excited oxygen. The pumping reaction

$$O_2(^1\Delta) + I \overset{k_F}{\rightarrow} O_2(^3\Sigma) + I^* \tag{5}$$

is countered by the reverse reaction

$$O_2(^3\Sigma) + I^* \overset{k_R}{\rightarrow} O_2(^1\Delta) + I \tag{6}$$

The equilibrium constant for these reactions is given by

$$k_{\text{eq}}(T) = (k_F/k_R) = 0.75\exp(401/T_{\text{cav}}) \tag{7}$$

With gain proportional to $([I^*] - \frac{1}{2}[I])$, Eq. (7) leads to the conclusion that there is a minimum amount of excited oxygen required to provide positive gain. This minimum is called the threshold yield Y_{th} given by

$$Y_{\text{th}} = \frac{1}{(1 + 2k_{\text{eq}})} = \frac{1}{[1 + 1.5\exp(401/T_{\text{cav}})]} \tag{8}$$

When power extraction reduces the excited oxygen density to Y_{th}, gain goes to zero and no more power can be extracted. Some of the excited oxygen energy is lost in flowing through the optical cavity as a result of deactivation before the energy is extracted by lasing. One example is the deactivation of I^* by water vapor after which another excited oxygen repumps the I atom. This reduces the energy pool by one $O_2(^1\Delta)$ and adds heat to the flow.

When the I_2 is mixed into the primary flow, the process may not provide contact between all of the excited oxygen and the I atoms. A condition where mixing is very poor is shown in Fig. 2. This effect will be accounted for with the parameter η_{mix}. Because the iodine parameter is the total flow into the device, the density of all iodine species is increased in the mixed region when mixing is poor, e.g., the density of I_2 goes to $[I_2]/\eta_{\text{mix}}$.

In experimental laser systems, there is typically an optical aperture placed in the cavity resonator system to define the height and width of the optical mode. This aperture may exclude portions of the flowfield and hence reduce power extraction. This loss is accounted for in the present model by the geometrical efficiency parameter η_{geo}.

Because of losses in optical extraction, such as diffraction, mirror scattering, and absorption, the optical extraction is not 100%. This will be accounted for with an optical extraction efficiency η_{ext}.

Finally, if power is extracted using a short, in the flow direction, resonator, another efficiency factor η_{res} is required to account for insufficient residence time to deplete the singlet delta oxygen to the minimum level.

Based on the preceding considerations, the heuristic equation for extracted optical power is given by

$$P_{\text{out}} = 91\dot{C}l_2 U_{Cl_2}[Y_{\text{plen}} - Y_{\text{th}} - Y_{\text{diss}} - Y_{\text{deact}}]\eta_{\text{mix}}\eta_{\text{geo}}\eta_{\text{ext}}\eta_{\text{res}} \tag{9}$$

This equation is not a derived equation. Rather, it is a method of macroscopically accounting for all phenomena in a COIL device that contribute to a reduced chemical efficiency. The Y terms following Y_{plen} represent $O_2(^1\Delta)$ energy that is not available for optical power extraction, each for different reasons as discussed earlier and later.

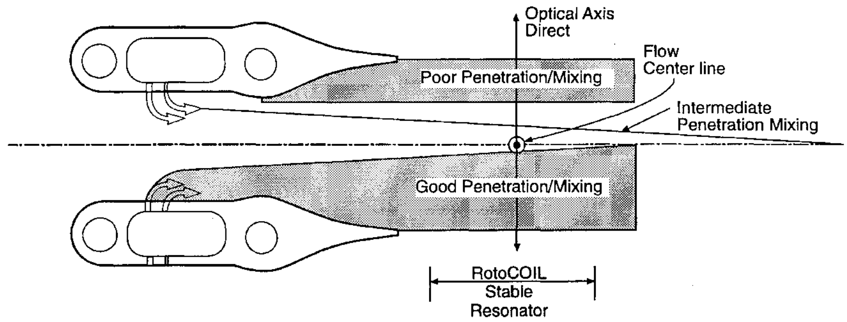

Fig. 2 RotoCOIL supersonic mixing nozzle, the penetration parameter qualitatively describes secondary flow penetration and mixing process in COIL. π = penetration parameter; $\pi = (\dot{n}_S/\dot{n}_P)\sqrt{(\overline{MW}_S T_S P_P/\overline{MW}_P T_P P_S)}$, where $\dot{n}$ = molar flow, $\overline{MW}$ = molecular weight, T = temperature, P = pressure, subscript P = primary flow, and subscript S = secondary injection flow.

In Eq. (9), Y_{plen} is introduced because it is customary to try to measure the $O_2(^1\Delta)$ just upstream of the nozzle. As will be discussed later, there are reaction losses and transport losses as the gas flows through the generator and ducts to the nozzle entrance.

From the preceding description, Y_{diss} is given by

$$Y_{\text{diss}} = \frac{N\dot{I}_2 F}{\dot{C}l_2 U_{Cl_2}\eta_{\text{mix}}} \tag{10}$$

where η_{mix} appears in the denominator because under poor mixing (Fig. 2), the local I_2 density is on the average larger by this factor.

The term Y_{th} depends on T_{cav} as well as the equilibrium rate constant, Eq. (8). When η_{mix} is less than unity, the heat generated during the dissociation process is not distributed throughout the flow. Thus the gas temperature in the mixed zone, where iodine species and therefore the gain reside, is greater than in the fully mixed condition. This is T_{cav} in Eqs. (7) and (8). Denoting ΔT_{diss} as the effect on gas temperature as a result of dissociation and T_{cavo} as the cavity gas temperature with no dissociation, one can give the effect of the added energy and η_{mix} by

$$T_{\text{cav}} = T_{\text{cavo}} + \frac{\Delta T_{\text{diss}}}{\eta_{\text{mix}}} \tag{11}$$

The term Y_{deact} can be estimated by integrating the deactivation rate over the cavity flow volume. For example, when the primary deactivator is H_2O, this term would be given by

$$Y_{\text{deact}} = \frac{\int^V K_{\text{deact}}[\text{I}^*][\text{H}_2\text{O}]\,\text{d}V}{\dot{C}l_2 U_{Cl_2}\eta_{\text{mix}}} \tag{12}$$

where $[\text{I}^*]$ is the actual I^* density during lasing, $[\text{H}_2\text{O}]$ is the water vapor density, and this integral is normalized to the oxygen flow to be consistent with the other terms.

Note that η_{ext} is the optical extraction efficiency for the gain medium that is consistent with the physics that gives rise to a particular value of η_{mix}. For a gain medium in which not all of the $O_2(^1\Delta)$ is accessed by the I containing part of the flow, the average density of I and I_2 species is greater than in the complete, uniformly mixed situation and T_{cav} is given by Eq. (11).

The flow residence time efficiency η_{res} is given by

$$\eta_{\text{res}} = 1 - e^{-L_m/x_{\text{ef}}} \tag{13}$$

The e-folding distance can be estimated by assuming that the operating gain in the mode is clamped at the threshold gain of the resonator. This assumption that gain is constant and some algebra gives

$$x_{\text{ef}} = \frac{Av^2\eta_{\text{mix}}}{2k_F N_A F\dot{I}_2 K_g} \tag{14}$$

where K_g is given by

$$K_g = 1 - (\text{I}^*/\text{I}_t)[1 - (1/k_{\text{eq}})] \tag{15}$$

With the assumption that gain is clamped to the resonator threshold gain G_{th}, the ratio of I^* to the total I atoms I_t is given by

$$\frac{\text{I}^*}{\text{I}_t} = \frac{1}{3}\left(1 + \frac{G_{\text{th}}}{\sigma(293/T_{\text{cav}})^{0.5}F[\text{I}_2]}\right) \tag{16}$$

Here the iodine number density $[\text{I}_2]$ is given by $\dot{I}_2 N_A/(Av\eta_{\text{mix}})$.

Using the Heuristic Equation

There are many ways the heuristic equation can be used to evaluate COIL data. An example is shown here that will then be applied to RotoCOIL data. The heuristic equation is a collection of parameters, some of which are very well known and some of which are not known at all. The known quantities for a given test data set are P_{out}, $\dot{C}l_2$, U_{Cl_2}, and $\dot{I}_2$, which are measured test parameters; η_{geo}, which is determined from the test hardware; and F, which has been measured for certain test conditions. Although Y_{plen} was measured during tests, the experimentally determined value has error and, as will be noted later, cannot always be trusted. Thus it will be treated as unknown.

The heuristic equation can be slightly rearranged to

$$\frac{P_{\text{out}}}{91\dot{C}l_2} = \eta_{\text{chem}} = U_{Cl_2}(Y_{\text{plen}} - Y_{\text{diss}} - Y_{\text{th}} - Y_{\text{deact}})\eta_{\text{mix}}\eta_{\text{geo}}\eta_{\text{ext}}\eta_{\text{res}} \tag{17}$$

This formulation shows all of the contributions to the global chemical efficiency parameter η_{chem} noted earlier.

In this paper, where data from the first seconds of a RotoCOIL test will be evaluated, Y_{deact} is very small compared with the other terms and thus will be neglected. Furthermore, for RotoCOIL, at the operating conditions to be evaluated later, x_{ef} is about 1.4 cm using the preceding equations. This, plus the geometry of the resonator used in RotoCOIL, gives an estimate of η_{res} of 0.997. For this paper then, η_{res} will be assumed to be unity. Rearrangement of Eq. (17), gathering together the known parameters, gives

$$\eta_{\text{mix}}(Y_{\text{plen}} - Y_{\text{th}}) = (K_1/\eta_{\text{ext}} + K_2 N) \tag{18}$$

where K_1 and K_2 are collections of knowns given by

$$K_1 = \frac{P_{\text{out}}}{91\dot{C}l_2 U_{Cl_2}\eta_{\text{geo}}} \tag{19}$$

and

$$K_2 = \frac{\dot{I}_2 F}{\dot{C}l_2 U_{Cl_2}} \tag{20}$$

The I_2 dissociation fraction F is treated as a known for purposes of this paper because it has been measured for conditions in RotoCOIL testing similar to what will be evaluated later.

Equation (18) is then a constraint equation on the unknowns Y_{plen}, N, Y_{th}, η_{mix}, and η_{ext}. Figure 3 shows an example of constraint curves for RotoCOIL-like test conditions for several values of outcoupled power to show the nature of the constraint. These constraint lines do not imply a causal relationship between Y_{plen} and η_{mix}. Rather, for a measured outcoupled power and for the values of N, T_{cav}, and η_{ext} assumed for these plots, the unknown parameters η_{mix} and Y_{plen} are pairwise determined by a point on the constraint line for that power.

The losses shown in the heuristic equation can be gathered together for the major components of a device, namely, the generator, the delivery ducting, the nozzle, and the resonator. For example, Y_{plen} depends upon generation efficiencies and ducting losses, η_{mix} is associated with the nozzle, and η_{geo} and η_{ext} are associated with

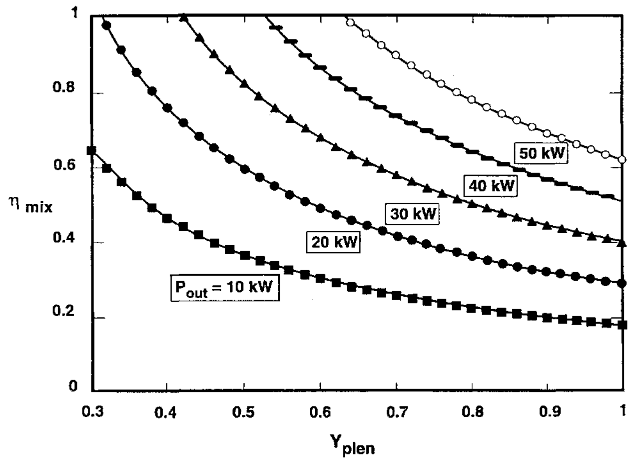

Fig. 3 Effect of P_{out} on heuristic constraint equation: N = 4, T_{cav} = 150 K, η_{ext} = 0.8, and η_{geo} = 0.9.

the resonator. Thus an evaluation of test data with the heuristic equation leads to an evaluation of the major device components. In the following section the heuristic equation will be used to evaluate a particular RotoCOIL test. The parameters N and T_{cav} will be obtained using an aerokinetics code, and η_{ext} will be determined by resonator properties, gain medium extraction characteristics, and extracted power saturation measurements. An upper limit to Y_{plen} will be determined using a generator and gas transport code. All of this will be used to determine the limit of parameter space that is consistent with the measured power.

III. RotoCOIL Assessment

The highest chemical efficiency for a large COIL device was 0.24 obtained in a RotoCOIL test; see Table 1. The best result to date was obtained in a test carried out Jan. 4, 1990, and designated test 0004HF8. This test has been selected for assessment because it demonstrated the best performance, and this should lead to the least error in partitioning losses.

RotoCOIL Description

The RotoCOIL device is briefly described next. A more complete description can be found in Ref. 4. The important features to this discussion are indicated next.

The oxygen generator consists of three rotary disk assemblies, the flow of which is combined and then passed through a cold trap to the nozzle. This configuration was selected for expediency, even though this large amount of ducting would be detrimental to performance. The generator/delivery system feeds an array of 42 supersonic nozzle blades where the I_2 is injected into the flow in the subsonic region as shown in Fig. 2. This injection upstream of the throat was selected to provide time for mixing and dissociation to take place upstream of the optical cavity. The nozzle array exit dimensions are 4.4 × 54.1 cm. The stable resonator consisted of a spherical mirror of radius 10 m and reflectivity 0.995 and one of several flat outcoupler mirrors having different reflectivities. For test 0004HF8, the outcoupler reflectivity was 0.85. The resonator mirrors were separated 3 m. The width of the optical mode L_m for this experiment was fixed by upstream and downstream aperture plates at 8 cm, and the vertical dimension of the mode was fixed by the 4-deg diverging cavity side walls. This cavity configuration in conjunction with the symmetric nature of a stable resonator prevented the mode from filling the full cavity flow area giving rise to an η_{geo} of 0.98. The mixing profiles generated by the 42 nozzle blades, including the cores and wakes, are averaged out by aligning the optical axis of the resonator across the nozzle array; see Fig. 2.

Test 0004HF8 Summary

Table 2 summarizes the pertinent data of test 0004HF8. There are separate data where appropriate for each of the three parallel generators. Except for the $O_2(^1\Delta)$ measurements, the values for each generator are very close. This indicates that the generators are operating very nearly the same. In view of this, the wide divergence of the $O_2(^1\Delta)$ measurements coupled with the failure of initial attempts to reconcile these measurements with the measured power lead to considering Y_{plen} as an unknown. Based on Table 2, the two constants K_1 and K_2 are 0.2900 and 0.0136, respectively. The term F was taken to be 0.95 based upon actual measurements made on RotoCOIL under very similar flow conditions. These constants give the general constraint conditions for test 0004HF8.

Table 2 Operating conditions for test 0004HF8

Parameters	Values
$\dot{C}l_2$, mole/s	1.692
$\dot{H}e_{primary}$, mole/s	7.540
$\dot{H}e_{secondary}$, mole/s	2.01
$\dot{I}_2$, mole/s	0.0206
U_{Cl_2}[a]	0.852, 0.850, 0.851
Y_{plen}[a]	0.439, 0.228, 0.530
T_{plen}[a], K	304, 321, 327
P_{plen}[a], torr	57.2, 57.2, 57.4
P_{cav}, torr	4.7
R_{out}	0.85
η_{geo}	0.98
P_{out}, kW[b]	37.2
η_{chem}	0.242

[a]Three measurements, one from each of the three generators.
[b]Average of 20 and 40 kJ calorimeters.

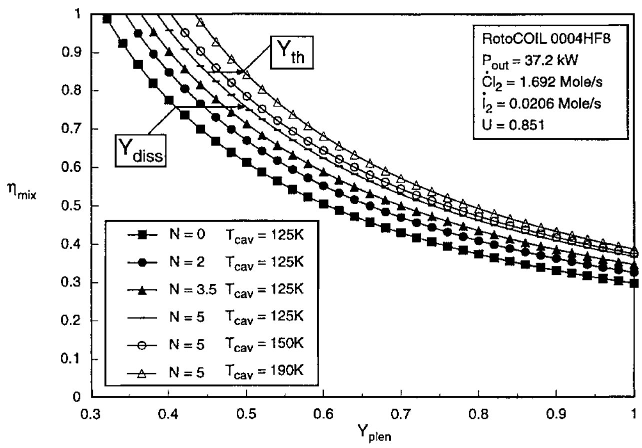

Fig. 4 Effect of N and T_{cav} on heuristic constraint equation: η_{ext} = 1.0 and η_{geo} = 0.9.

Figure 4 shows a number of constraint lines based upon these constants. The lowest line is with $N = 0$, $T_{cav} = 125$ K, and $\eta_{ext} = 1.0$. As stated earlier, N must be at least 2 from energy considerations; η_{ext} can be no bigger than 1 by definition. An isentropic flow calculation for this nozzle (area ratio 2) and these flow conditions with no water vapor condensation gives a T_{cav} of about 125 K. This is the lowest T_{cav} can be because the flow is not isentropic. Therefore, the lowest curve on Fig. 4 defines the lower bound for Y_{plen}. The next three lines are N = 2, 3.5, and 5 with the other conditions the same. These lines indicate the sensitivity of the constraint line to N. The next two lines are for $N = 5$, $\eta_{ext} = 1$, and $T_{cav} = 150$ and 190 K, respectively, to indicate the sensitivity of the constraint curve to T_{cav}.

To provide better estimates for N and T_{cav} for test 0004HF8, a series of calculations using the one-dimensional RECOIL aerokinetic code[11] were conducted; the results are given in Table 3. The RECOIL model premixes the primary and secondary flows, conserving enthalpy, and calculates the aerokinetic processes from the subsonic region through the throat and into the cavity. The full COIL kinetic rate package of Ref. 12 was used in this calculation. For the premixed model to work, the baseline rate constant of 7 × 10^{-15} cm^3/mol-s for the production of the intermediate species I_2^* in the iodine dissociation process by $O_2(^1\Delta) + I_2$ is adjusted by a dissociation rate multiplier of 90–100 to match existing dissociation data. These results show that N is about 4.7 when there is no water

Table 3 One-dimensional RECOIL aerokinetic code calculations for T_{cav} and N for test 0004HF8 flow conditions with varying water flow rate (plenum yield = 0.6)

Dissociation rate multiplier	Water flow rate, mole/s	I_2 diss. fract.	N	Nozzle exit plane T, K	P, torr	M	Mode midpoint T, K	P, torr	M
90	0.00	0.95	4.7	161	5.0	2.0	164	4.4	2.0
0	0.16	0.0	0.0	157	5.0	2.0	150	4.1	2.1
100	0.16	0.95	5.7	167	5.2	2.0	173	4.8	2.0

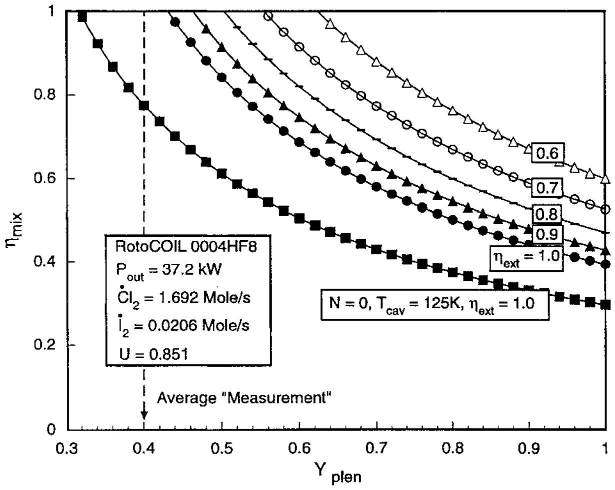

Fig. 5 Effect of η_{ext} on heuristic constraint equation: $N = 6$, $T_{cav} = 170$ K, and $\eta_{geo} = 0.98$.

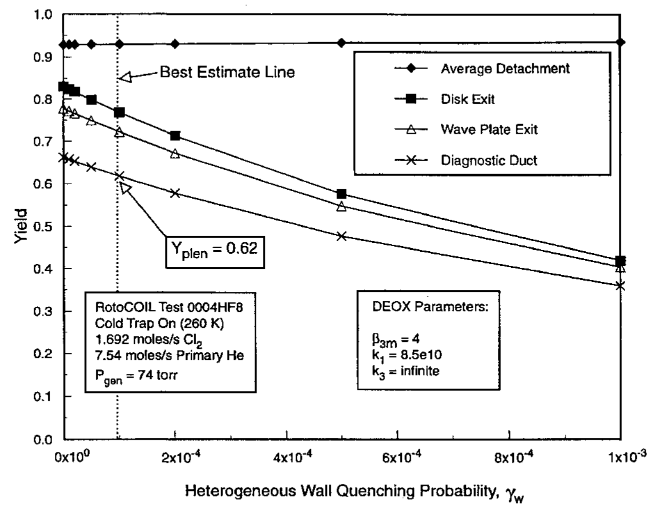

Fig. 6 Effect of heterogeneous wall quenching probability γ_w on RotoCOIL generator/delivery yield profile.

vapor present. For RotoCOIL, the temperature conditions in the generator and cold traps are such that the water partial pressure is on the order of 1–2 torr at the nozzle plenum. This corresponds to a molar flow rate of approximately 0.16 mole/s for test 0004HF8. Under such conditions, N increases as a result of water deactivation of I* and excited I_2 during the dissociation process. These code simulations indicate that N is increased to at least 5.7 including only the kinetic effects of water. The cavity temperature at the mode midpoint is predicted to increase from 150 K with no dissociation to 173 K including water and dissociation effects. The predicted cavity pressure at the mode midpoint of 4.8 torr compares very favorably with the measured cavity pressure from taps along the optical cavity wall of 4.7 torr, which substantiates the conclusion that T_{cav} must be greater than the isentropic value of 125 K.

Figure 5 shows a series of constraint lines to show the sensitivity to η_{ext}. The lowest is again the lowest line on Fig. 4. The next line up is for $N = 6$, $T_{cav} = 170$, and $\eta_{ext} = 1.0$. The successive lines upwards are for $\eta_{ext} = 0.9, 0.8, 0.7$, and 0.6. The separation of the lowest and next lowest lines represents the estimate of the combined loss as a result of Y_{diss}, dissociation loss, and Y_{th}, threshold yield, based upon code and experimental results. Also shown in Fig. 5 is the average measured value of Y_{plen} for this test. Clearly it is outside the boundary of any constraint line, especially in view of the fact that η_{ext}, as will be discussed later, is significantly less than 1. This is why Y_{plen} is being treated as an unknown, as discussed earlier.

At this point the actual combination of the remaining unknowns η_{mix}, Y_{plen}, and η_{ext} must lie somewhere in the region of Fig. 5 that is above and to the right of the constraint line labeled $\eta_{ext} = 1$. However, Y_{plen} must be substantially less than 1 because there is substantial ducting between the generator and the nozzle and the yield parameter at the generator cannot be greater than 1. In the next section the loss during generation and ducting to the nozzle will be evaluated. Following that, η_{ext} will be evaluated.

Generation and Transport

To estimate the generation and transport losses of $O_2(^1\Delta)$ from the RotoCOIL rotating disk generator and delivery system, the DEOX code developed by Crowell[13] was used. This code couples a two-dimensional wetted wall reactor model to a one-dimensional aerokinetic transport model to describe the evolution of $O_2(^1\Delta)$ (hence Y_{plen}) for the RotoCOIL generator and delivery system. Reference 14, which presents an analytic solution to this problem, gives a comprehensive review of the COIL generator/delivery modeling approach, associated set of rates, and other modeling parameters that are used in the DEOX code and a critique regarding how well these parameters are known. The DEOX model, which gives a numerical solution to the same governing partial differential equations, is used in the present study to remove the uncertainties associated with the approximations used to develop the analytic result of Ref. 14. As discussed in Ref. 14, not all of the relevant rate constants are known. The uncertainties associated with chlorine utilization were eliminated in the present analysis by setting the parameters that affect this process so that the code results match the measured utilization of 0.85 in test 0004HF8. Two parameters in DEOX directly affecting the production of $O_2(^1\Delta)$ that are largely unknown are the $O_2(^1\Delta)$ production rate k_3 and the heterogeneous deactivation rate γ_w for $O_2(^1\Delta)$ on the liquid basic hydrogen peroxide surface in the generator. To obtain an upper bound of Y_{plen}, k_3 was set to infinity and a set of DEOX calculations were made varying γ_w. Predictions of yield at various locations through the generator/delivery system are presented in Fig. 6, including at the BHP liquid surface (detachment yield), at the disk exit, and at the RotoCOIL diagnostic duct where yield measurements were made. Using $k_3 = \infty$ and $\gamma_w = 0$ gives from Fig. 6 the highest upper bound for Y_{plen} of 0.66. In general, the data do not support a value for γ_w of zero. An estimate of 5×10^{-5} is suggested by Ref. 15 for ducting. A higher value is expected on BHP-coated surfaces. For purposes of a more reasonable upper bound than 0.66, a value of 1×10^{-4} is selected here. This gives from Fig. 6 a best estimate upper bound of 0.62. Both the absolute and best estimate upper bound for Y_{plen} are plotted on the constraint curve in Fig. 7. The shaded area in Fig. 7 represents the constraints on parameters from arguments presented thus far.

Extraction Efficiency

To evaluate extraction efficiency η_{ext} and to determine the dependence of the extraction efficiency on the mixing efficiency η_{mix}, a heuristic expression for extraction efficiency was utilized. It is based

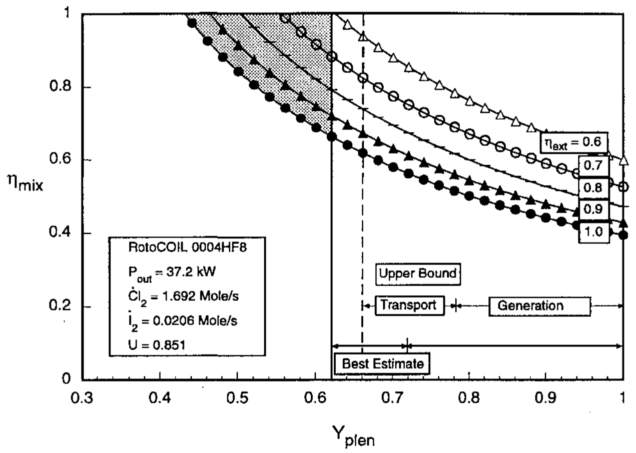

Fig. 7 **Effect of Y_{plen} bounding analysis on heuristic solution space (defined by light gray area): $N = 6$, $T_{cav} = 170$ K, and $\eta_{geo} = 0.98$.**

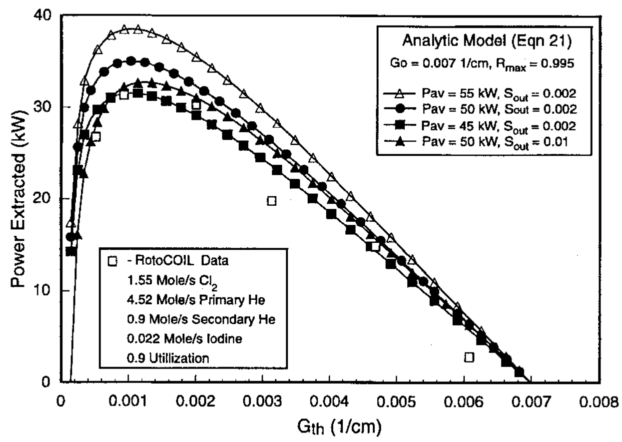

Fig. 8 **η_{ext} determined from heuristic extraction efficiency analysis of RotoCOIL power saturation data.**

on the assumption that a COIL device responds to photon flux like a Rigrod laser. This is not strictly true because, in Rigrod lasers, the gain species is the same as the energy containing species, and so power is extracted directly as the gain saturates. In a COIL device, however, because energy transfers from the $O_2(^1\Delta)$ to the iodine lasing species, the power is extracted indirectly with gain saturation. Nevertheless, as will be seen from experimental data, the saturation characteristics of RotoCOIL are described quite closely by a Rigrod-like saturation curve. The COIL extraction efficiency is expected to be somewhat higher than that determined by a Rigrod-type analysis for reasons to be described.

The heuristic power extraction efficiency is developed as a product of the basic Rigrod extraction efficiency η_{extm}, times the extraction efficiency of the resonator η_{extr}. Thus the outcoupled power is given by

$$P_{out} = P_{av}\eta_{ext} \tag{21}$$

where

$$\eta_{ext} = \eta_{extm}\eta_{extr} \tag{22}$$

and

$$\eta_{extm} = 1 - G_{th}/G_0 \tag{23}$$

Because all of the power that is extracted from the gain medium is not in the output beam

$$\eta_{extr} = \frac{P_{out}}{P_{out} + \text{all other losses}} \tag{24}$$

In the preceding, G_{th} is the threshold gain of the resonator:

$$G_{th} = \frac{-\ell n(R_{out}R_{max})}{2L_g} \tag{25}$$

The other losses in Eq. (25) include the mirror scattering and absorption losses, the power out of R_{max}, and diffraction losses. In this analysis, the mirror reflectivities and scattering coefficients are treated as measured quantities, but because the diffraction losses were not measured, an analytic estimate made in Appendix A of Ref. 16 is used. A nonsaturable distributed loss is not considered in the gain region in this analysis because the estimated diffraction and mirror scattering losses are seen to be sufficient to explain the measured power saturation data for RotoCOIL.

Treating the diffraction loss as a fraction $\mathcal{P}$ of the outcoupled power, η_{extr} is given by

$$\eta_{extr} = \frac{(1 - R_{out} - S_{out})}{(1 - R_{out} - S_{out})(1 + \mathcal{P}) + S_{out} + (R_{out}/R_{max})^{\frac{1}{2}}(A_{max}/A_{out})(1 - R_{max} - S_{max} + S_{max})} \tag{26}$$

The two S_{max} terms are retained for illustrative purposes. The factor $(R_{out}/R_{max})^{1/2}$ accounts for the fact that the flux at R_{max} is somewhat less than at R_{out} and the factor A_{max}/A_{out} accounts for the larger beam footprint at R_{max} because the resonator is half symmetric. For the present resonator configuration, A_{max}/A_{out} is estimated to be 1.06. The terms S_{out} and S_{max} are the scattering coefficients at R_{out} and R_{max}, respectively, and can include absorption loss if comparable.

To develop a bounding estimate of η_{ext}, the heuristic extraction efficiency model is compared with available RotoCOIL saturation data. Figure 8 presents experimental power saturation data as a function of threshold gain for a series of RotoCOIL tests with the R_{out} mirror varied[5] as well as a series of analytic predictions from Eq. (21). These data are for average flow conditions as given on the figure that were very similar, but not identical, to test 0004HF8. The parameters that need to be specified in Eq. (21) to generate a power prediction include P_{av}, G_o, R_{out}, S_{out}, and $\mathcal{P}$. An average G_o of 0.007 cm^{-1} was determined by visually extrapolating the experimental saturation data of Fig. 8 to the zero power location on the threshold gain axis. Lasing ceases at this point because threshold gain has increased to G_o. Using the analytically derived diffractive loss $\mathcal{P}$ variation with R_{out} from Ref. 16 leaves P_{av}, R_{out}, and S_{out} to be specified. From scattering and reflectivity measurements conducted on similar optics to test 0004HF8, it is believed that R_{out} and S_{out} can be no better than 0.995 and 0.002, respectively. The bounding analysis consists of successively varying P_{av} and S_{out} to just match the experimental saturation curve with the results given in Fig. 8. The top three curves (open triangle, solid circle, and solid square) show the effect of successive reductions in P_{av} from 55 to 45 kW with S_{out} fixed at 0.002. The peak extraction efficiency for each of these curves is 0.7. The 50-kW prediction is seen to fully encompass the full set of experimental data, thus providing an upper bound on η_{ext}. Reducing P_{av} to 45 kW causes the prediction to match the peak experimental data point, but the rolloff in the prediction with lower threshold gain is underpredicted, indicating there are higher resonator losses in the experimental data compared with the prediction. By increasing the resonator loss for $P_{av} = 50$ kW to $S_{out} = 0.01$, a very good match with the experimental data is made both in terms of magnitude and profile. The predicted extraction efficiency for this case dropped to 0.65.

An adjustment must now be made to this bounding estimate for $\eta_{ext} = 0.70$ to account for the differences between COIL and Rigrod saturation characteristics. A reasonable assumption is made that the difference between the two estimates resides in the medium extraction term only. Manipulating the simplified saturation model derived by Crowell and Plummer,[14] one can show that the medium

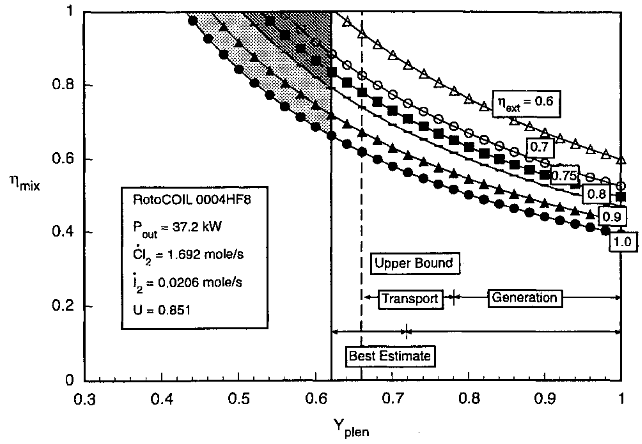

Fig. 9 Effect of η_{ext} bounding analysis on reducing the heuristic solution space (identified by dark gray area): N = 6, T_{cav} = 170 K, and η_{geo} = 0.98.

extraction efficiency for COIL $(\eta_{extm})_{COIL}$ is simply the product of the Rigrod medium extraction efficiency $(\eta_{extm})_{Rigrod}$ and the factor

$$(\eta_{extm})_{COIL} = (\eta_{extm})_{Rigrod}\left[\frac{1}{1-\phi G_{th}/G_o}\right] \tag{27}$$

where ϕ is a COIL chemistry parameter that varies between 0 and 1 and is given as a function of Y_{cav}, which is $Y_{plen} - Y_{diss}$, Y_{th}, and k_{eq} by

$$\phi = \frac{(k_{eq}-1)(Y_{cav}-Y_{th})}{1+Y_{cav}k_{eq}-Y_{cav}} \tag{28}$$

Taking into account the range of uncertainty in Y_{cav} and T_{cav} for test 0004HF8, ϕ is bounded between 0.55 and 0.75. Using $\phi = 0.65$ as the average of this uncertainty range together with an assumed 20% increase in G_o to account for test 0004HF8 flow differences from those for Fig. 8 gives the multiplying factor as 1.138, which provides the upper bound estimate for $(\eta_{ext})_{COIL}$ equal to 0.80. This value is plotted on Fig. 9 and closes in the bounding triangle for parameter space for test 0004HF8.

Dependence of η_{ext} on η_{mix}

The form of the heuristic equation basically assumes that η_{ext} does not depend upon η_{mix}. This is not quite true, but it will be shown here that for the values of η_{mix} that fit into the parameter space for test 0004HF8 this is a very good approximation. When η_{mix} is less than unity, the potential effect on extraction efficiency is through the effect of gain dependence on two factors, Y_{cav} and T_{cav}. First, the dependence of gain on Y_{cav}, the $O_2(^1\Delta)$ yield in the laser cavity, and T_{cav} is determined starting from the definition of gain given by

$$G_o = \sigma(293/T_{cav})^{\frac{1}{2}}\left([I^*] - \tfrac{1}{2}[I]\right) \tag{29}$$

As noted earlier, there is an equilibrium between I^*, $O_2(^1\Delta)$, and $O_2(^3\Sigma)$ given by

$$\frac{[I^*]}{[I]} = \frac{k_{eq}[O_2(^1\Delta)]}{O_2(^3\Sigma)} \tag{30}$$

Combining Eq. (29) with Eq. (30) gives, after some algebra,

$$G_o = \sigma\left(\frac{293}{T_{cav}}\right)^{\frac{1}{2}}[I_2]F\left[\frac{(1+2k_{eq})Y_{cav}-1}{(k_{eq}-1)Y_{cav}+1}\right] \tag{31}$$

where

$$Y_{cav} = Y_{plen} - \frac{N\dot{I}_2F}{\dot{C}l_2U_{Cl_2}\eta_{mix}} \tag{32}$$

where σ is equal to 7.5×10^{-18} cm^2 and $[I_2]$ is the I_2 density per cubic centimeter. When η_{mix} does not equal unity, the effective I_2 density is $[I_2]/\eta_{mix}$.

However, the region in the nozzle flow that has gain is reduced by η_{mix}. Thus the average G_o in one nozzle flow is made up of two gain regions, one that is $\eta_{mix}d$ wide having a gain $(G_o)_{\eta_{mix}}$, where d is the nozzle exit width, and a region $d(1-\eta_{mix})$ where there is no I_2 and therefore no gain. From this the average G_o is given across each nozzle and therefore across the entire gain length as

$$\bar{G}_o = \frac{\eta_{mix}d(G_o)_{\eta_{mix}} + d(1-\eta_{mix})(0)}{d} = (G_o)_{\eta_{mix}}\eta_{mix} \tag{33}$$

Because $(G_o)_{\eta_{mix}}$ is just G_o from Eq. (31) divided by η_{mix} (because $[I_2]$ is replaced by $[I_2]/\eta_{mix}$) in this simple two-zone model, the average G_o is the G_o given by Eq. (31), with Y_{cav} given by Eq. (32) but with T_{cav} as determined next.

When η_{mix} is less than 1, the heat of dissociation is delivered to less of the flow. This increases the temperature in this portion of the flow compared with the fully mixed situation. Thus T_{cav} in this region is higher. Because this is the region where there is gain, the T_{cav} in Eq. (30) is higher, depending on η_{mix}. Aerodynamic code analysis (Table 3) shows that the heat of dissociation increases T_{cav} when fully mixed, from 150 to 173 K for $N = 5.7$. Therefore T_{cav} in the gain equation is scaled by $T_{cav} = 150\,\mathrm{K} + 23/\eta_{mix}$.

From the preceding, G_o and therefore η_{extm} and η_{ext} depend on η_{mix} through Y_{diss} and T_{cav}. Figure 10 shows the dependence of G_o, the dependence of η_{extm} (the higher curve), and the dependence of the overall η_{ext} (the lower curve) on η_{mix}, which includes the resonator extraction efficiency for RotoCOIL with $R_{out} = 0.85$. As can be seen, for η_{mix} greater than 0.5, η_{ext} is essentially constant; thus assuming η_{ext} to be independent of η_{mix} is legitimate in the heuristic equation for values of η_{mix} that are in the parameter space for test 0004HF8.

Results

Based on the preceding analysis and discussion, the partition of the losses in test 0004HF8 is summarized in Table 4 for a point at the center of the solution space given in Fig. 9 (dark triangle). The results in Table 4 can be distributed to the major components,

Table 4 Chemical efficiency loss accounting for RotoCOIL test 0004HF8 using midpoint of heuristic solution space

Location	Loss parameter	Normalized power in flow
Generator entrance	——	1.0
BHP film interface	$U_{Cl_2} = 0.851$	0.851
	$Y_{detach} = 0.90$	0.766
Generator exit	$Y_{exit} = 0.74$	0.630
Delivery	$Y_{plen} = 0.59$	0.502
Nozzle	$Y_{diss} = 0.086$	0.429
	$Y_{th} = 0.059$	0.379
	$\eta_{mix} = 0.94$	0.356
Resonator	$\eta_{geo} = 0.98$	0.349
	$\eta_{ext} = 0.70$	0.244
η_{chem}	——	0.244

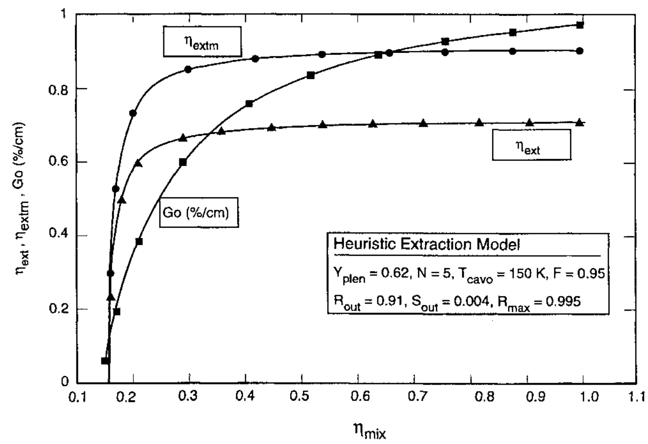

Fig. 10 Effect of η_{mix} on η_{ext} from the heuristic extraction efficiency model.

Table 5 Distribution of losses by major COIL device components

Device component	Percentage loss	Comment
Generator	37.0	Includes internal transport loss but no water losses
Delivery	12.8	——
Nozzle	14.6	Includes water loss (1.5% for increased N and 2.7% for increased $T_{\rm cav}$) but no gain effects
Resonator	11.2	Includes $\eta_{\rm geo}$
Power out	24.4	——

as shown in Table 5. Note that the results in Table 4 are based on a detachment yield of 0.90. This value is in agreement with other experimental data.[17]

Clearly the largest contributor to losses is the combination of generation and transport losses, which represent over half of the total loss. The rest of the losses are about half and half between nozzle and extraction. Some of the losses, i.e., the minimum dissociation loss ($N = 2$ compared with 0) and $Y_{\rm th}$ for $T_{\rm cav}$ up to 125 K, are unavoidable consequences of the physics of the laser.

IV. Summary and Conclusions

A number of conclusions can be drawn regarding the nature of the losses (reduction in overall chemical efficiency) in the RotoCOIL device. Some of the observations, particularly for the oxygen generator, are sufficiently general that they apply to any type of oxygen generator that is based on the reaction of gaseous chlorine with liquid basic hydrogen peroxide and, therefore, indicate the direction to be taken to improve device performance.

RotoCOIL

From the values summarized in Table 5, the oxygen generator (including wave plate separator) is the RotoCOIL component with the highest loss (37.0%). Note that the chemistry loss is 23.4% ($U_{\rm Cl_2} = 0.851$ and $O_2(^1\Delta)$ detachment yield is 0.90), whereas the internal transport loss is 15.6%. The nozzle mixing and resonator losses are comparable, 14.6 and 11.2%, respectively. The ducting loss is moderate, in comparison, 12.8%, but when the generator internal transport loss is added to the ducting loss, transport losses, 28.4%, are the largest single contribution to loss in the RotoCOIL device.

The average of the measured values of $O_2(^1\Delta)$ during the RotoCOIL test 0004HF8 was too low to be correct. Figure 5 shows that the average value just does not fit into the parameter space. This was true of other RotoCOIL tests as well. Nominal experimental error bars of $\pm 20\%$ would still leave the measurement out of the parameter space, despite the fact that the diagnostic instrumentation was carefully calibrated. This discrepancy is unexplained.

The nozzle injection and mixing losses in RotoCOIL are deduced to be modest, not the primary source of loss. Also, the RotoCOIL power extraction efficiency is in line with expectations for a device of this gain length, 54 cm, given the mirror scatter and diffraction losses.

General Conclusions

Based on the RotoCOIL evaluation, there are some conclusions that are more general and would apply to other devices. This evaluation indicates that at the RotoCOIL generator flow and pressure regime of about 75 torr, the generator chemistry is rather effective, namely, detachment yield of about 90% and utilization of 85%. The detachment yield deduced here is in agreement with other experimental data. Furthermore, these experiments have shown that increasing the disk pack rotation rate above 20 rpm (the RotoCOIL nominal) to 30–40 rpm increases utilization above 90% with no detrimental effect on yield. Thus, the basic physics and chemistry of the reaction of chlorine with basic peroxide are quite effective in producing $O_2(^1\Delta)$ in large quantities. The mixing of I_2 into the subsonic entry plenum of a supersonic nozzle also is quite effective in this flow and pressure regime. It is suggested that although mixing is not perfect, there is not a lot of room for improvement.

Future Directions

These results also indicate the direction that further efforts to improve COIL performance need to take for the major elements of a COIL device.

Generator

Generally higher-pressure operation will result in a reduced impact of water vapor because it will reduce its molar fraction in the flow. Also, increased pressure will make generators smaller, which is required to minimize ducting losses while feeding nozzles at higher pressure. There will be benefits realized from generator concepts where the surface film temperature is colder to further reduce the impact of water vapor. Care must be taken to not reduce $O_2(^1\Delta)$ and $U_{\rm Cl_2}$ in the process. Also, increasing the ratio of BHP flow/Cl_2 flow would be beneficial in maintaining fresher BHP to the Cl_2 flow, thus elevating $U_{\rm Cl_2}$ and possibly $O_2(^1\Delta)$ yield simultaneously. Clearly, the internal volume of generators must be made smaller to reduce internal transport losses.

Ducting

Along with volume reduction within the generator, care must be taken to design only the absolute minimum of ducting from the generator to the nozzle. This becomes even more important at high-pressure operation. In other words, get the nozzle as close to the generator as physically possible.

Nozzle/Mixing

As generators are improved by working at higher pressures, nozzle design must follow suit. Injection hole size, patterns, and distance from the throat need to be optimized for higher flow and pressures. The I_2 dissociation processes and rate constants need to be affirmed to aid in analyzing changes required by higher-pressure operation. Also, as devices become larger, i.e., gain length becomes longer, greater care in designing the supersonic expansion contours of the nozzle, the optical cavity, and the nozzle/cavity interface to minimize cavity pressure (density) variations will be required.

Resonator/Power Extraction

Generally larger devices will lead to reduction of extraction losses. Taller nozzles will increase $\eta_{\rm geo}$. With longer gain length, extraction efficiency will be increased, possibly sufficient to permit lower I_2 flows. This would reduce dissociation losses, which in turn would result in somewhat lower cavity temperatures because of reduced heat added to the flow by dissociation. Lower cavity temperatures would reduce the $Y_{\rm th}$ loss. These would be relatively small effects individually but in concert could be significant, especially with reduced impact of water vapor, which is very detrimental to performance, when operating at higher generator pressure.

References

[1]Hager, G. D., Watkins, L. J., Meyer, R. K., Johnson, D. E., Bean, L. J., and Loverro, D. L., "A Supersonic Oxygen-Iodine Laser," U.S. Air Force Weapons Lab., AFWL-TR-87-45, Kirtland AFB, NM, Jan. 1988.

[2]Berg, J. O., Brock, J. C., Clendening, C. W., Coleman, W. B., English, W. D., Harpole, G. M., Horowitz, A. B., Lewis, D. H., Miller, D. J., Trost, J. E., and Wonica, D., "Oxygen-Iodine Supersonic Technology," U.S. Air Force Weapons Lab., AFWL-TR-85-43, Vols. 1–3, Kirtland AFB, NM, Oct.1988.

[3]Dickerson, R., private communication, Rockwell International/Rocketdyne, Canoga Park, CA, Nov. 1993.

[4]Truesdell, K. A., Healey, K. P., Miller, J. A., Hanko, L., Keating, P., and Hager, G. D., "The Design and Construction of a 25-kW Rotating Disk Chemical Oxygen-Iodine Laser (RotoCOIL)," U.S. Air Force Phillips Lab., PL-TR-92-1035, Kirtland AFB, NM, Dec. 1992.

[5]Truesdell, K. A., Miller, J. A., Keating, P., and Hanko, L., "RotoCOIL Power Extraction Experiments," *Laser Digest*, U.S. Air Force Weapons Lab., WL-TR-89-46, Kirtland AFB, NM, Jan. 1990, pp. 136–148.

[6]Hon, J., private communication, Rockwell International/Rocketdyne, Canoga Park, CA, Nov. 1993.

[7]Azyazov, V. N., Zagidullin, M. V., Nikolaev, V. D., Svistun, M. I., and Khvatov, N. A., "Oxygen-Iodine Laser with a Drop-Jet Generator of $O_2(^1\Delta)$ Operating at Pressures up to 90 Torr," *Soviet Journal of Quantum Electronics*, Vol. 25, No. 5, 1995, pp. 418–420.

[8]Truesdell, K. A., private communication, U.S. Air Force Phillips Lab., Kirtland AFB, NM, Nov. 1993.

[9]Elior, A., Barmashenko, B. D., Lebiush, E., and Rosenwaks, S., "Experiment and Modelling of a Small Scale Supersonic Oxygen-Iodine Chemical Laser," *Applied Physics B*, Vol. 61, No. 1, 1995, pp. 37–47.

[10]Helms, C. A., Hanko, L., Healey, K. P., Murdough, M., and Phipps, S. P., "Construction and Performance of a 5 Centimeter Gain Length Supersonic COIL," U.S. Air Force Phillips Lab., PL-TR-95-1055, Kirtland AFB, NM, March 1995.

[11]Crowell, P. G., "RECOIL: A One-Dimensional Chemical Oxygen Iodine Laser Performance Model," Logicon RDA, Rept. 87-A/K-3-02-1079, Albuquerque, NM, Nov. 1989.

[12]Perram, G. P., and Hager, G. D., "The Standard Chemical Oxygen-Iodine Laser Kinetics Package," U.S. Air Force Weapons Lab., AFWL-TR-88-50, Kirtland AFB, NM, Oct. 1988.

[13]Crowell, P. G., "DEOX: A Two-Dimensional Wetted Wall Singlet Delta Oxygen Generator and Delivery Duct Model," Logicon RDA, Rept. 87-A/K-03-02-1149, Albuquerque, NM, Jan. 1990.

[14]Crowell, P. G., and Plummer, D. N., "Simplified Chemical Oxygen Iodine Laser (COIL) System Model," *Intense Laser Beams and Applications*, edited by W. E. McDermott, Proceedings of the SPIE 1871, SPIE—The International Society for Optical Engineering, Bellingham, WA, 1993, pp. 148–180.

[15]Crannage, R. P., Dorko, E. A., Johnson, D. E., and Whitefield, P. D., "Surface Deactivation Efficiencies for $O_2(^1\Delta)_{(g)}$ on a Range of Materials: I. Pyrex, Nickel, Copper, Nickel-Copper Alloy and Nickel," *Chemical Physics*, Vol. 169, 1993, pp. 267–273.

[16]Hon, J., Plummer, D. N., Crowell, P. G., Erkkila, J., Hager, G. D., Helms, C., and Truesdell, K. A., "A Heuristic Method for Evaluating COIL Performance," AIAA Paper 94-2422, June 1994.

[17]Harpole, G. M., Berg, J. O., English, W. D., Horowitz, A. B., and Record, J. R., "Basic Hydrogen Peroxide (BHP) Flow Experiment," U.S. Air Force Weapons Lab., WL-TR-89-88, Vols. 1 and 2, Kirtland AFB, NM, March 1990.